

CRISPR/dCas-mediated gene activation toolkit development and its application for parthenogenesis induction in maize

Xiantao Qi^{1,2}, Huimin Gao¹, Renyao Lv¹, Wenbo Mao¹, Jinjie Zhu^{1,2}, Changling Liu¹, Long Mao¹, Xinhai Li^{1,2} and Chuanxiao Xie^{1,2,*}

¹Institute of Crop Science, Chinese Academy of Agricultural Sciences, National Key Facility for Crop Gene Resources and Genetic Improvement, Beijing 100081 China

²Hainan Yazhou Bay Seed Lab, Hainan Province 572024 China

*Correspondence: Chuanxiao Xie (xiechuanxiao@caas.cn)

<https://doi.org/10.1016/j.xplc.2022.100449>

ABSTRACT

Clustered regularly interspaced short palindromic repeats (CRISPR)-Cas systems can be engineered as programmable transcription factors to either activate (CRISPRa) or inhibit transcription. Apomixis is extremely valuable for the seed industry in breeding clonal seeds with pure genetic backgrounds. We report here a CRISPR/dCas9-based toolkit equipped with dCas9-VP64 and MS2-p65-HSF1 effectors that may specifically target genes with high activation capability. We explored the application of *in vivo* CRISPRa targeting of maize *BABY BOOM2* (*ZmBBM2*), acting as a fertilization checkpoint, as a means to engineer parthenogenesis. We detected *ZmBBM2* transcripts only in egg cells but not in other maternal gametic cells. Activation of *ZmBBM2* in egg cells *in vivo* caused maternal cell-autonomous parthenogenesis to produce haploid seeds. Our work provides a highly specific gene-activation CRISPRa technology for target cells and verifies its application for parthenogenesis induction in maize.

Key words: CRISPRa, *ZmBBM2*, egg cell, apomixis engineering, maternal haploid

Qi X., Gao H., Lv R., Mao W., Zhu J., Liu C., Mao L., Li X., and Xie C. (2023). CRISPR/dCas-mediated gene activation toolkit development and its application for parthenogenesis induction in maize. *Plant Comm.* **4**, 100449.

INTRODUCTION

Apomictic crop breeding using embryos directly arising from egg cells (ECs) allows the fixation and indefinite propagation of a desired maternal genotype (Yao et al., 2018). Maternal haploid induction resulting from parthenogenesis—embryo formation without the paternal genome—has long been sought in breeding. Haploid inducers harboring mutations (Gilles et al., 2017; Kelliher et al., 2017; Liu et al., 2017) that cause sperm genome instability (Li et al., 2017; Jiang et al., 2022; Sun et al., 2022) have been utilized for haploid breeding in diverse crops, including rice (Yao et al., 2018), maize (Dong et al., 2018), wheat (Liu et al., 2020), tomato (Zhong et al., 2022), millet (Cheng et al., 2021), and legumes (Wang et al., 2022). By contrast, *BABY BOOM* (BBM) transcription factors can function as male-expressed embryogenic triggers, suggesting that the spatial and temporal regulation of *BBM* expression in ECs could be exploited to engineer parthenogenesis, as demonstrated for *OsBBM1* in rice (Khanday et al., 2019). To achieve this goal in maize, we selected endogenous *ZmBBM2* as the engineering target based on its evolutionary relationship with *OsBBM1* (Supplemental Figure 1).

Clustered regularly interspaced short palindromic repeats (CRISPR)-associated nucleases have been devised in which a single guide RNA (sgRNA) guides the assembly of a transcriptional activator (CRISPRa) or inhibitor effectors at selected loci (Gilbert et al., 2013; Qi et al., 2013; Chavez et al., 2015; Konermann et al., 2015). Although several CRISPRa tools have been described (Tanenbaum et al., 2014; Chavez et al., 2015; Konermann et al., 2015), *in vivo* CRISPRa has not been characterized in maize, let alone used in ECs. The objectives of this study were to establish a robust CRISPRa system in maize and, further, to engineer parthenogenesis through CRISPRa-mediated targeting of *ZmBBM2* *in vivo* in the maize EC. Our data and protocols presented herein provide a robust maize CRISPRa system as an alternative method to engineer parthenogenesis for breeding and a potent alternative for genome editing through the EC.

Published by the Plant Communications Shanghai Editorial Office in association with Cell Press, an imprint of Elsevier Inc., on behalf of CSPB and CEMPS, CAS.

RESULTS AND DISCUSSION

Robust maize CRISPRa screening in mesophyll protoplasts

We developed six sets of vectors based on dCas9 (Figure 1A). For the first strategy, the fusion effector consisted of a single activation domain from *Arabidopsis* (*Arabidopsis thaliana*) ETHYLENE RESPONSE FACTOR2 (Li et al., 2013), VP64, or nuclear factor- κ B *trans*-activating subunit p65 (Essen et al., 2009). For the second strategy, we included the modified sgRNA scaffold sgRNA 2.0, containing MS2-binding RNA aptamers (Konermann et al., 2015), to recruit an additional transcriptional activator besides VP64 (ETHYLENE RESPONSE FACTOR-heat-shock factor 1 [HSF1], p65-HSF1, or VP64-HSF1), which we fused to the activation domain of human HSF1 (Marinho et al., 2014) for domain synergy. dCas9-VP64 and the other transcriptional activators were translated as large proteins that were self-cleaved from the included T2A peptide to release NLS-dCas9-VP64, which can directly bind to the sgRNA scaffold and NLS-MS2-effector-HSF1 (Figure 1A and 1B).

We then tested these CRISPRa systems by targeting the maize *DPS1* gene, which exhibits low expression in leaves (Vauterin et al., 1999). We designed an sgRNA specific for a region 100 bp upstream of the *ZmDPS1* transcription start site (TSS) (Figures 1B and 1C; Supplemental Table 1) and introduced these constructs into maize leaf mesophyll protoplasts. All CRISPRa systems yielded at least 1.6-fold increases in transcript levels, indicative of transcriptional activation (Figure 1D). The CRISPRa5 system produced the most robust transcriptional activation (>11-fold versus the control). To further optimize the activation window of CRISPRa5, we targeted four potential promoter regions upstream of the *ZmDPS1* TSS: the 5' untranslated region and the regions 1–100, 100–200, and 200–300 bp upstream of the TSS. Again, the sgRNA targeting the region 1–100 bp upstream of the *ZmDPS1* TSS gave the strongest activation (Figure 1E). Then, targeting of regions 1–100 bp upstream of three other genes, *ZmTrxh*, *Embryo sac2*, and *Root cap protein1* (Figure 1F–1H), was tested and showed 375.4-, 5.3-, and 4.5-fold activation in our system. Therefore, targeting a region 100 bp upstream of the TSS with CRISPRa5 resulted in strong transcriptional activation in maize cells.

Transient CRISPRa5 editing in EC protoplasts

To explore the potential for EC engineering, we established a simple protocol for isolation and micromanipulation of single female gametic cells (Figure 2A–2H and Supplemental Figure 2). We isolated female gametic cells by microdissection under a stereomicroscope and enzymatically digested the ovule tissues for 1 h to isolate whole embryo sacs. We manually separated the antipodal cells, synergid cells, central cells, and ECs under a stereomicroscope, with a success rate of approximately 25% of the young kernels. We prepared ECs and protoplasts from a previously developed DFP line that harbors a stable transgene encoding the red fluorescent protein DsRed2 driven by the barley aleurone-specific *Lipid transfer protein2* (*Ltp2*) promoter (Dong et al., 2018). We modified CRISPRa5 with the EC-specific *DD45* promoter from *Arabidopsis* (Steffen et al., 2007) and an sgRNA to activate *LTP2pro:DsRed2* in ECs from DFP plants (Figure 2I). We transiently transfected EC protoplasts

with the CRISPRa5^{pLTP2} plasmid targeting *LTP2pro:DsRed2* via electroporation and examined DsRed2 fluorescence. Three individuals out of 20 cells showed notable red fluorescence, indicating that the *LTP2pro:DsRed2* cassette was transcriptionally activated, leading to DsRed2 translation and observed fluorescence (Figure 2J). By comparison, out of the hundred control ECs transfected with the non-targeting plasmid, none (0/100) showed fluorescence.

Our data thus suggest that isolated EC protoplasts can be subjected to transient transformation and genome editing. The EC shows great promise as a target for engineering, as isolated ECs largely behave as true protoplasts (Kranz and Lörz, 1993) with an active and open chromatin state in maize (Chen et al., 2017) that is thus accessible for manipulation. Multiple steps critical to sexual reproduction have been successfully achieved *in vitro* with isolated cells, such as fertilization (Kranz and Lörz, 1993), gamete fusion (Peng et al., 2005), and zygote engineering (Toda et al., 2019), and can even lead to fertile regenerated plants (Kranz and Lörz, 1993; Toda et al., 2019; Maryenti et al., 2021). Therefore, our data suggested that the modification of ECs may allow for heritable engineering and regeneration of fertile plants, as *in vitro* fertilization and embryo rescue are feasible in maize.

In vivo ectopic activation of *ZmBBM2* in ECs

The *in vitro* positive results encouraged us to attempt to engineer parthenogenesis by activating *ZmBBM2* in ECs *in vivo*. We generated *CRISPRa5^{BBM}* constructs targeting *ZmBBM2* (Figure 3A) and stably transformed them into the maize inbred line ZC01 via *Agrobacterium*-mediated transformation. Nine independent transgenic lines were obtained. To exclude the effects of *CRISPRa5^{BBM}* copy-number variation, we performed droplet digital PCR (ddPCR) assays and selected five T₃ lines from independent transformants (EA15, EA19, EA22, EA34, and EA36) that carried single-copy transgenes (Figure 3B). Reverse-transcription ddPCR (RT-ddPCR) with *Zmelf4a* as the reference (Supplemental Figure 3) revealed up to 10³ copies of *CRISPRa5^{BBM}* (Figure 3C) and *ZmBBM2* per 1 μ g total RNA (Figure 3D) from isolated ovaries of all nine *CRISPRa5^{BBM}* lines, but copies were not detected in wild-type ZC01. We selected EA19 for further characterization, as it demonstrated the best *ZmBBM2* activation.

We then quantified transcript levels in single antipodal cells, synergid cells, central cells, and ECs from EA19 plants isolated by micromanipulation. As expected, single-cell RT-ddPCR detected *CRISPRa5^{BBM}* and *ZmBBM2* transcripts only in ECs (Figure 3E) in the 10-fold diluted RNA pool from 10 lysed cells (Hashimoto-Torii et al., 2014), indicating that *ZmBBM2* transcription was specifically activated in ECs because of *CRISPRa5^{BBM}* expression. We examined dCas9 protein and *ZmBBM2* mRNA in ovaries by *in situ* hybridization (with an mRNA probe complementary to *ZmBBM2* or an anti-FLAG antibody for 3 \times FLAG-dCas9), confirming the targeted activation of *ZmBBM2* transcription in ECs before fertilization (Figure 3F). Even though parthenogenesis bypasses fertilization between sexual gametes, another fertilization event between two central cells (polar nuclei) and sperm is needed for endosperm and seed formation. We thus examined *CRISPRa5^{BBM}* and *ZmBBM2*

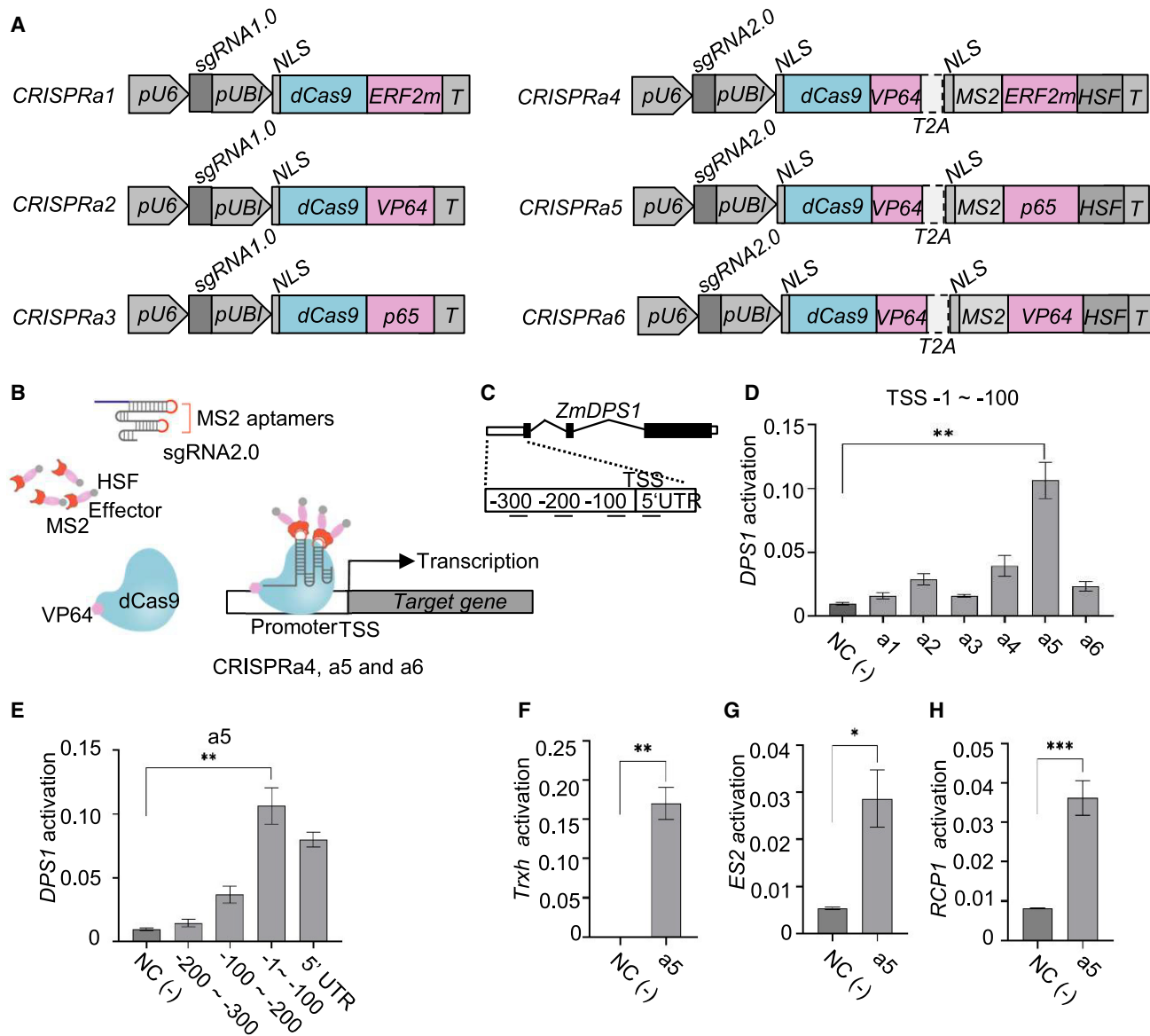


Figure 1. Evaluating transcriptional activation of CRISPRa (a1–a6) constructs in maize mesophyll protoplasts.

(A) Core components of the CRISPRa vectors. dCas9, *Streptococcus pyogenes* Cas9 lacking endonuclease activity (mutations D10A, H840A); ERF2m, modified transcriptional activator from *Arabidopsis* ETHYLENE RESPONSE FACTOR2; HSF, human heat-shock factor 1; MS2, bacteriophage coat proteins; NLS, nuclear localization signal; P65, NF- κ B *trans*-activating subunit P65; pU6, *ZmPoIII* U6-2 promoter; pUBI, maize *Ubiquitin1* promoter; sgRNA1.0, routine sgRNA of Cas9; sgRNA2.0, sgRNA scaffold containing two MS2 stem loops; T, terminator; T2A, insect virus *Thosea asigna* self-cleaving peptide (18 amino acids); VP64, four copies of the herpes simplex virus early transcriptional activator VP16.

(B) Schematic diagram of the three components of the a4–a6 systems with MS2 connected to the transcriptional activation P65 and HSF1.

(C and D) Activated *ZmDPS1* expression, as determined by qRT-PCR.

(C) Schematic diagram of the *ZmDPS1* locus. The first transcription start site was designated as +1.

(D) Fold activation of *ZmDPS1* expression when the sgRNA targets the sequence between –1 and –100 from the transcription start site using a1–a6. The maize *Ubiquitin* gene (NCBI GenBank: U29159.1) was used as the reference. Relative expression levels were calculated using the $2^{-\Delta C_t}$ (threshold cycle) method.

(E) Fold activation of *ZmDPS1* expression as a function of sgRNA location with the a5 system.

(F–H) Validation of the a5 system with the genes **(F)** *ZmTrxh*, **(G)** *ZmES2*, and **(H)** *ZmRCP1*, which have low transcript abundance in maize mesophyll protoplasts.

All values are means \pm SEM with $n = 3$ biological replicates. An unpaired *t*-test was used to determine significant differences (* $p < 0.05$, ** $p < 0.01$, *** $p < 0.001$).

expression in isolated ovaries from selfed EA19 ears at 0 to 9 days after pollination by RT-ddPCR. *ZmBBM2* expression rapidly increased after pollination relative to that in the wild type (Figure 3G and 3H).

Engineered CRISPRa5 produces parthenogenesis phenotypes

To investigate parthenogenesis in *CRISPRa5^{BBM}* lines, we examined immature embryo development before fertilization

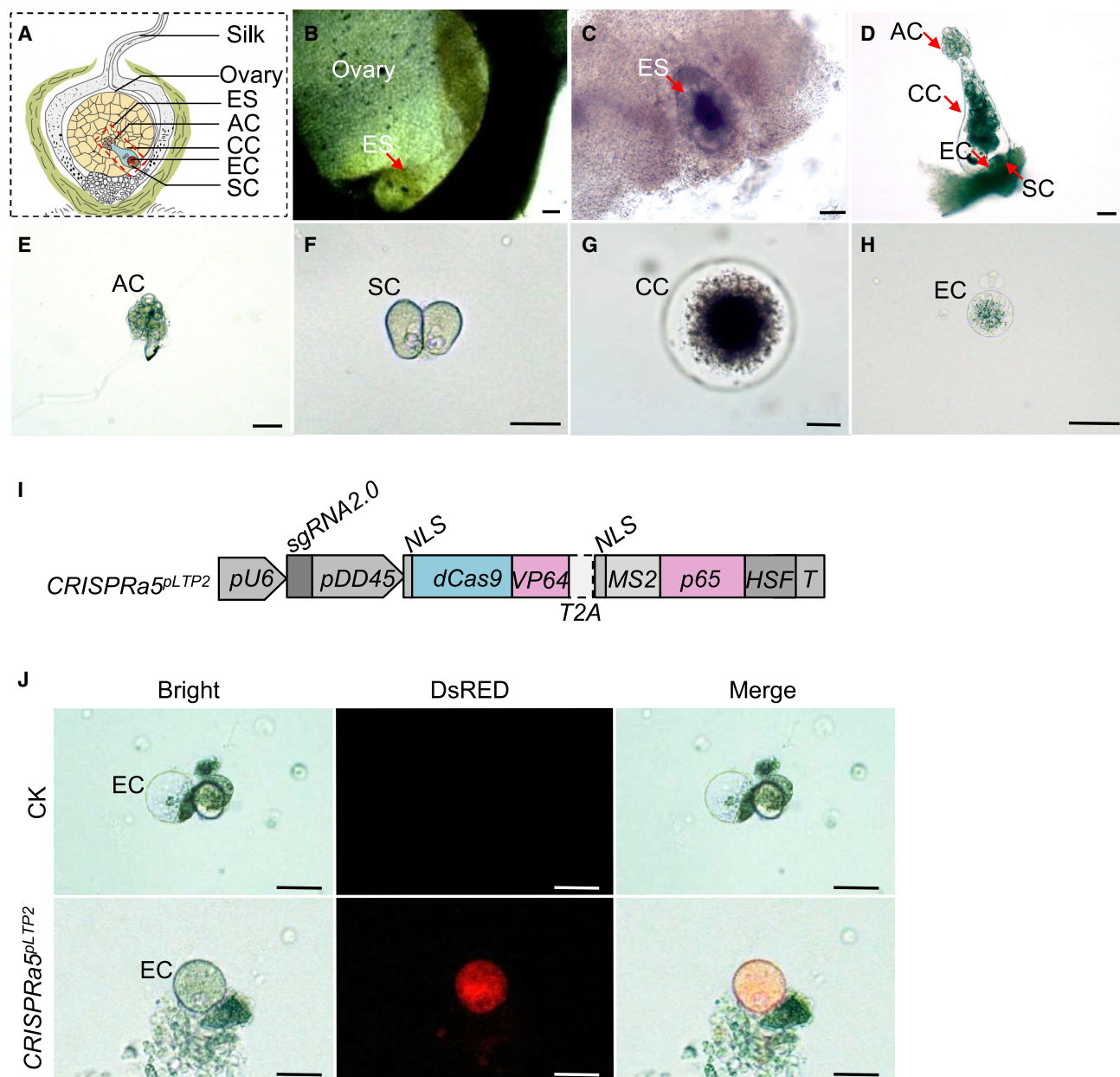


Figure 2. Isolation of single female gamete cells and verification of the CRISPRa5 system in egg cell (EC) protoplasts.

(A–H) Micromanipulation and isolation of maize female gamete cells at the single-cell level.

(A) Schematic diagram of maize ovary structure. AC, antipodal cell; CC, central cell; EC, egg cell; ES, embryo sac; SC, synergid cell.

(B) Isolated maize ovary showing the exposed ES (red arrow).

(C) Manual micromanipulation to separate the ES from the ovary under a stereomicroscope.

(D) Obtaining single cells from the ES via partial enzymatic digestion.

(E–H) Isolated ACs (E), SCs (F), CCs (G), and ECs (H).

(I and J) Targeted activation of a stably transformed aleurone-specific *DsRED* cassette expressed in the EC *in vitro*. The DFP line was previously constructed and harbors a *DsRED* expression cassette driven by the barley aleurone-specific *LTP2* promoter (Dong et al., 2018).

(I) Schematic diagram of the CRISPRa5 vector targeting *LTP2pro:DeRed2* with an effector cassette driven by the EC-specific promoter of *Arabidopsis* *DD45* (Steffen et al., 2007).

(J) Ectopic expression of *DsRED* in an isolated EC, as revealed by DsRED fluorescence.

The vector (I) plasmid was delivered into the EC via electroporation, and fluorescence was observed 24 h after transient transformation. The DsRED signals were detected under a confocal microscope. Bright, brightfield. Bars: 50 μ m.

(Figure 4A). Notably, 3.9% of EA19 kernels developed double embryo sacs in ovaries. To evaluate the haploid generation rate, we used the DFP line as the pollen donor to sort haploid

seeds: the lack of GFP indicates that an embryo developed as a maternal clone (Dong et al., 2018) (Figure 4B). We confirmed the fluorescence patterns in seeds using confocal microscopy

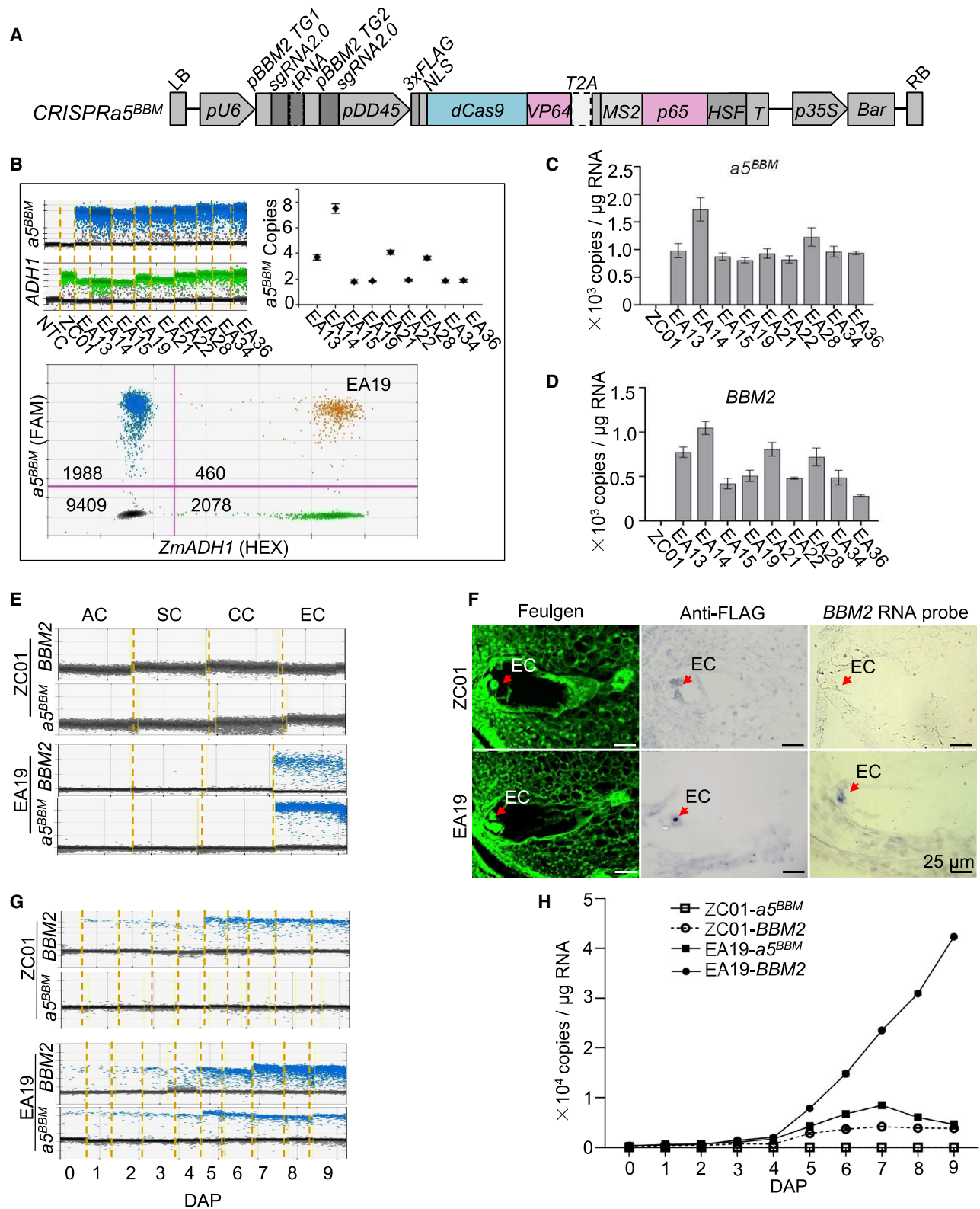


Figure 3. Targeted activation of *ZmBBM2* in egg cells *in vivo*.

(A) Constructed vector of *CRISPRa5^{BBM2}* (*a5^{BBM2}*). 3×FLAG, 3 tandem FLAG epitope tags; Bar, *BlpR* gene. Other components are the same as those shown for *CRISPRa5* in Figure 1A.

(B) ddPCR identification of transformed copy numbers. The nine independent transformants were EA13, EA14, EA15, EA19, EA21, EA22, EA28, EA34, and EA36 in the T₃ generation. The *a5^{BBM2}* amplitudes were scored with the FAM probe, and *ZmADH1* reference amplitudes were scored with the HEX

(legend continued on next page)

(Supplemental Figure 4) and grew sorted haploid kernels to verify their ploidy levels and examine their morphology (Figure 4C). The haploid plants were thinner and smaller, with sterile male and female flowers, compared with their diploid siblings and the wild type. We confirmed the ploidy levels by flow cytometry using isolated nuclei from mesophyll protoplasts, and the signal intensity values in the haploids were approximately half those of the diploid (Figure 4D). All nine *CRISPRa5^{BBM}* lines generated 0.4% to 3.55% haploid kernels, with most producing 1.5% to 2% haploid kernels (Figure 4E). These values were similar to the haploid induction rate caused by *MTL/ZmPLA1/NLD* (Liu et al., 2017). The production of double embryo sacs before fertilization and haploids without the use of inducer pollen suggests that CRISPRa-engineered parthenogenesis is maternally cell autonomous, unlike the effect of loss-of-function mutations in inducers (Gilles et al., 2017; Kelliher et al., 2017; Liu et al., 2017; Yao et al., 2018; Zhong et al., 2019, 2020; Li et al., 2021; Wang et al., 2022). Moreover, ectopic BBM expression using constitutive promoters could induce additional pleiotropic phenotypes, including neoplastic growth, hormone-free regeneration of explants, and alterations in leaf and flower morphology (Boutillier et al., 2002). By contrast, we precisely activated *BBM* expression only in ECs, potentially avoiding these negative pleiotropic effects.

In summary, our work provides a precise and highly specific gene activation CRISPRa technology for target cells in maize. It also provides an additional approach for maternally derived seed production and double haploid breeding that may be applicable to other crops.

METHODS

CRISPRa5^{BBM} vector construction

Details about CRISPRa construction, elements, and targets and evaluation of transcriptional activation in maize cells are provided in the Supplemental methods.

To obtain the *CRISPRa5^{BBM}* vector, the *Arabidopsis DD45* promoter was amplified and assembled into the CUB vector using in-fusion cloning with a pEASY-Uni Seamless Cloning and Assembly Kit (TransGen Biotech, Beijing, China). The two sgRNA2.0s, pBBM2 TG1 sgRNA2.0 and pBBM2 TG2 sgRNA2.0, were designed to target regions upstream of the TSS (36 or 166 bp). pBBM2 TG1 sgRNA2 and pBBM2 TG2 sgRNA2.0 were connected by the sequence of the *Arabidopsis* Gly transfer RNA (*At-tRNA^{Gly}*). All primers used in this study are listed in Supplemental Table 3.

Isolation of single gametic cells

Our previously developed DFP line (Dong et al., 2018) and the *CRISPRa5^{BBM}* line generated in this study were used as plant materials.

probe. Top left panel, amplitudes of the targets and the reference; top right panel, calculated *a5^{BBM}* copy numbers; bottom panel, typical droplets with the *a5^{BBM}*, *ZmADH1*, and *a5^{BBM}/ZmADH1* amplitudes and blank amplitudes (left lower quadrant) of line EA19 plotted in four quadrants separated by two vertical crossing red lines. The corresponding droplet numbers are shown in each quadrant.

(C–F) Quantification of gene expression in non-pollinated female gametophytes.

(C and D) mRNA expression level of *a5^{BBM}* (C) and *ZmBBM2* (D) were scored in isolated ovaries. Quantifications were converted into expressed copy numbers per 1 µg total RNA. Each sample used 20 ovaries for RNA extraction.

(E) ddPCR identification of mRNA expression among isolated ECs, ACs, SCs, and CCs from line EA19.

(F) *In situ* hybridization identification of *a5^{BBM}* and *BBM2* expression in egg cells *in vivo*. Feulgen staining was used to visualize ovule development. Immunohistochemical assays with alkaline phosphatase-labeled anti-FLAG antibody or *BBM2* RNA probe were used for *a5^{BBM}* and *ZmBBM2* detection, respectively.

(G and H) *ZmBBM2* and *a5^{BBM}* mRNA expression time course from 0 to 9 days after pollination in the embryo sac. Each sample used 20 embryo sacs for RNA extraction.

Ears were bagged before silk emergence, and the husks were surface sterilized with 70% (v/v) ethanol. Ovules were dissected from the ears when the silk emergence length was between 5 and 15 cm before or after pollination. Protocols for isolation of single gametic cells and *in vitro* manipulation of ECs are provided in the Supplemental methods.

CRISPRa5^{BBM} and *ZmBBM2* expression in ovaries

The ovary was separated by peeling the ovary wall under RNase-free conditions. Three biological replicates were collected, each consisting of 20 ovaries for each experimental group. Total RNA isolation, quality control, and cDNA synthesis were performed as described by the manufacturer (Vazyme BioTech, Jiangsu, China). Candidate primers and probes for the amplification of *dCas9*, *ZmBBM2*, and *Zmelf4 α* were designed using Primer3Plus. All primers and probes are listed in Supplemental Table 3. Each ddPCR sample contained 11 µL 2× ddPCR Supermix for Probes (no dUTP) (Bio-Rad, Hercules, CA, USA), 900 nM each primer pair, and 227 nM probe, to which 2 µL first-strand cDNA was added; the final volume was adjusted to 22 µL with sterile ddH₂O. The droplet counts were analyzed, and absolute gene expression measurements were generated using Bio-Rad QuantaSoft software (v.1.6.6.0320) with default settings for threshold determination to distinguish positive and negative droplets.

CRISPRa5^{BBM} and *ZmBBM2* expression at the single-cell level

Synergid cells, antipodal cells, central cells, ECs, and central cells were isolated under a microscope as described in the main text. Single-cell equivalents were generated using 1/10 of a pool of 10 lysed cells for the RNA template. First-strand cDNA synthesis was performed using a One-Step RT ddPCR Advanced Kit for Probes (Bio-Rad). Primers for candidate genes and probes for amplification of *dCas9* and *ZmBBM2* were designed using Primer3Plus. Each ddPCR sample contained 5 µL SuperMix, 2 µL reverse transcriptase, 1 µL DDT, 900 nM each primer pair, and 250 nM probe, to which 1 µL RNA template was added; the final volume was adjusted to 20 µL with sterile ddH₂O. The reactions were run on a QX200 AutoDG Droplet Digital PCR System according to the instruction manual (Bio-Rad). The droplet counts were analyzed, and absolute gene expression measurements were generated using Bio-Rad QuantaSoft software (v.1.6.6.0320) with default settings for threshold determination to distinguish positive and negative droplets.

Methods and protocols for Feulgen staining, *in situ* hybridization using immunohistochemistry, and mRNA are also provided in the Supplemental methods.

Determination of the parthenogenesis phenotypes of multiple embryo sacs

The *CRISPRa5^{BBM}* line in the EA19 background was inspected to determine the ratio of multiple embryo sacs versus non-pollinated kernels from ears at silk emergence lengths between 5 and 15 cm. Sixty non-pollinated kernels each from the middle parts of three ears of different plants were carefully picked and manually stripped to reveal the ovaries. The ovary wall was removed under a stereomicroscope (Nikon, SMZ1500, Tokyo, Japan). The wall-free ovaries were processed for Feulgen staining as described above. Single or multiple embryo sacs

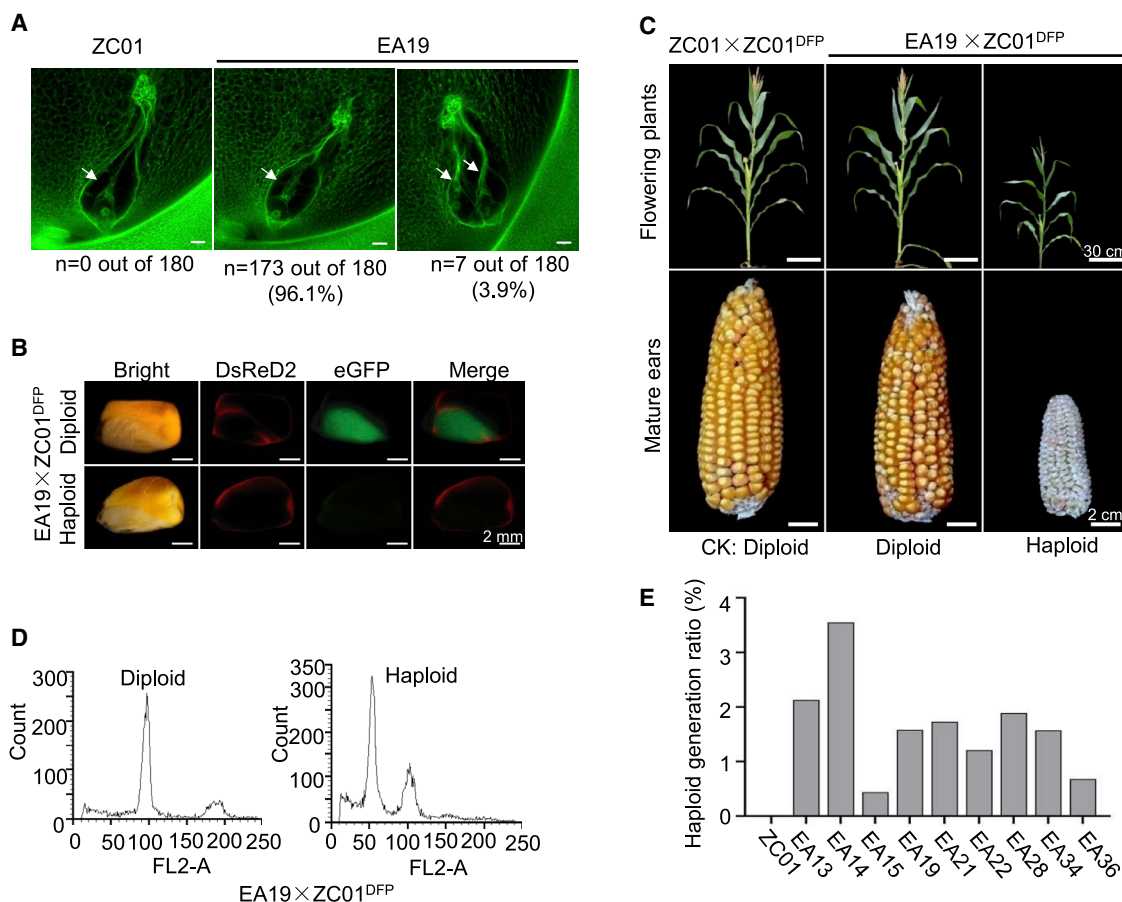


Figure 4. Apomixis phenotypes caused by the targeted activation of *BBM2* in vivo.

(A) Double embryo sacs in EA19 ovaries. Bars: 50 μ m.

(B–E) Efficiency of maternal haploid generation in engineered lines.

(B) Screening of maternal haploid kernels produced from the cross EA19 × ZC01^{DFP}.

(C) Representative flowering plants and mature ears.

(D) Cell DNA contents in haploid plants (right) and control diploid plants (left) determined by flow cytometry.

(E) Efficiency of haploid generation across nine *CRISPRa5^{BBM}* lines.

with positive Feulgen staining were observed under a Zeiss microscope (LSM700, Jena, Germany) using brightfield (control) and a 488-nm excitation wavelength at 10 × 10 magnification.

Efficiency of maternal haploid seed production

For maternal haploid screening, the dual fluorescent protein DFP method was performed as previously described (Dong et al., 2018). In brief, when the aleurone layer showed red fluorescence for DsRed2 but the embryo did not produce green fluorescence from EGFP, the embryo was determined to be haploid and derived from a maternal EC only. The wild-type inbred line ZC01, nine *CRISPRa5^{BBM}* lines, and DFP plants were grown in the greenhouse. During flowering, DFP plants were selected as pollen donors and used to pollinate all other genotypes. After maturation, the resulting ears and kernels were subjected to haploid screening using fluorescent patterns. The haploid and diploid maize kernels were identified using a LUYOR-3415RG light source (LUYOR, Shanghai, China) with a 488-nm excitation filter for EGFP and/or a 520-nm excitation filter for DsRed2. Haploid grain numbers out of the total number of grains per line were used to calculate haploid frequency.

Ploidy identification

Flow cytometry was performed to determine the ploidy levels of cells as previously described (Dong et al., 2018). In brief, putative haploid seeds

along with diploid control seeds were germinated and the seedlings grown to the three-leaf stage. Approximately 1 g young leaf tissue was collected, sliced with a razor blade, and filtered through an 80- μ m nylon mesh. After centrifugation at 1000 r/min and 4°C for 5 min, the pellet was re-suspended in 1 mL OTTO I buffer (100 mM citric acid, 0.5% [v/v] Tween 20 [pH 2.0]) and 2 mL OTTO II buffer (400 mM Na₂HPO₄ [pH 8]) and stained with 50 μ L 1.5 mM propidium iodide in the dark for 20 min. The ploidy levels were analyzed on a FACSCalibur system (BD, Franklin Lakes, NJ, USA). The data were extracted with Cell Quest software (BD) and analyzed using ModFit (Yerity Software House, Topsham, ME, USA).

Imaging and fluorescence observation

Photographs of plant morphology and kernels were captured with a Canon 70D camera (Canon, Tokyo, Japan). The kernels from the ears of diploid maize and *CRISPRa5^{BBM}* × DFP haploid plants were identified with a DFP-1 fluorescence flashlight (Electron Microscopy Sciences, Hatfield, PA, USA) using a 554-nm excitation wavelength with a DsRed2-specific filter and a 488-nm excitation wavelength with an EGFP-specific filter (Dong et al., 2018). Longitudinal sections of haploid and diploid maize seeds were visualized using a 554-nm excitation wavelength with a DsRed2-specific filter and a 488-nm excitation wavelength with an EGFP-specific filter under a Nikon stereomicroscope (SMZ1500) at 10 × 0.75 magnification. Images of samples stained with Feulgen were

obtained under a confocal laser scanning microscope (Zeiss LSM700) with a 488-nm excitation wavelength and an EGFP-specific filter. The immunohistochemistry and mRNA *in situ* hybridization samples were observed using a DM1000 LED system (Leica, Wetzlar, Germany) with brightfield at 10 × 10 magnification.

SUPPLEMENTAL INFORMATION

Supplemental information is available at *Plant Communications Online*.

AUTHOR CONTRIBUTIONS

Conceptualization, C.X. and X.Q.; investigation, X.Q., H.G., R.L., W.M., J.Z., C.L., L.M., X.L., and C.X.; writing – original draft, C.X., X.Q., and L.M.; writing – review & editing, C.X. and X.Q.; funding acquisition, C.X. and X.Q.; supervision, C.X. and X.L.

ACKNOWLEDGMENTS

This research was supported by the National Science Foundation of China (32001551 and 31771808), the China Postdoctoral Science Foundation (2020M680779), the Agricultural Science and Technology Innovation Program of the CAAS (S2022ZD03), and Hainan Yazhou Bay Seed Laboratory (B21HU0215).

DECLARATION OF INTERESTS

A patent related to this study has been submitted.

Received: July 1, 2022

Revised: August 15, 2022

Accepted: September 9, 2022

Published: September 12, 2022

REFERENCES

- Boutillier, K., Offringa, R., Sharma, V.K., Kieft, H., Ouellet, T., Zhang, L., Hattori, J., Liu, C.M., Van Lammeren, A.A.M., Miki, B.L.A., et al.** (2002). Ectopic expression of BABY BOOM triggers a conversion from vegetative to embryonic growth. *Plant Cell* **14**:1737–1749.
- Chavez, A., Scheiman, J., Vora, S., Pruitt, B.W., Tuttle, M., P R Iyer, E., Lin, S., Kiani, S., Guzman, C.D., Wiegand, D.J., et al.** (2015). Highly efficient Cas9-mediated transcriptional programming. *Nat. Methods* **12**:326–328.
- Chen, J., Strieder, N., Krohn, N.G., Cyprys, P., Sprunck, S., Engelmann, J.C., and Dresselhaus, T.** (2017). Zygotic genome activation occurs shortly after fertilization in maize. *Plant Cell* **29**:2106–2125.
- Cheng, Z., Sun, Y., Yang, S., Zhi, H., Yin, T., Ma, X., Zhang, H., Diao, X., Guo, Y., Li, X., et al.** (2021). Establishing in planta haploid inducer line by edited SiMTL in foxtail millet (*Setaria italica*). *Plant Biotechnol. J.* **19**:1089–1091.
- Dong, L., Li, L., Liu, C., Liu, C., Geng, S., Li, X., Huang, C., Mao, L., Chen, S., and Xie, C.** (2018). Genome editing and double-fluorescence proteins enable robust maternal haploid induction and identification in maize. *Mol. Plant* **11**:1214–1217.
- van Essen, D., Engist, B., Natoli, G., and Sacconi, S.** (2009). Two modes of transcriptional activation at native promoters by NF- κ B p65. *PLoS Biol.* **7**:e73.
- Gilbert, L.A., Larson, M.H., Morsut, L., Liu, Z., Brar, G.A., Torres, S.E., Stern-Ginossar, N., Brandman, O., Whitehead, E.H., Doudna, J.A., et al.** (2013). CRISPR-mediated modular RNA-guided regulation of transcription in eukaryotes. *Cell* **154**:442–451.
- Gilles, L.M., Khaled, A., Laffaire, J.B., Chaignon, S., Gendrot, G., Laplaige, J., Bergès, H., Beydon, G., Bayle, V., Barret, P., et al.** (2017). Loss of pollen-specific phospholipase NOT LIKE DAD triggers gynogenesis in maize. *EMBO J.* **36**:707–717.
- Hashimoto-Torii, K., Torii, M., Fujimoto, M., Nakai, A., El Fatimy, R., Mezger, V., Ju, M.J., Ishii, S., Chao, S.-H., Brennand, K.J., et al.** (2014). Roles of heat shock factor 1 in neuronal response to fetal environmental risks and its relevance to brain disorders. *Neuron* **82**:560–572.
- Jiang, C., Sun, J., Li, R., Yan, S., Chen, W., Guo, L., Qin, G., Wang, P., Luo, C., Huang, W., et al.** (2022). A reactive oxygen species burst causes haploid induction in maize. *Mol. Plant* **15**:943–955. <https://doi.org/10.1016/j.molp.2022.04.001>.
- Kelliher, T., Starr, D., Richbourg, L., Chintamanani, S., Delzer, B., Nuccio, M.L., Green, J., Chen, Z., McCuiston, J., Wang, W., et al.** (2017). MATRILINEAL, a sperm-specific phospholipase, triggers maize haploid induction. *Nature* **542**:105–109.
- Khanday, I., Skinner, D., Yang, B., Mercier, R., and Sundaresan, V.** (2019). A male-expressed rice embryogenic trigger redirected for asexual propagation through seeds. *Nature* **565**:91–95.
- Konermann, S., Brigham, M.D., Trevino, A.E., Joung, J., Abudayyeh, O.O., Barcena, C., Hsu, P.D., Habib, N., Gootenberg, J.S., Nishimasu, H., et al.** (2015). Genome-scale transcriptional activation by an engineered CRISPR-Cas9 complex. *Nature* **517**:583–588.
- Kranz, E., and Lörz, H.** (1993). *In vitro* fertilization with isolated, single gametes results in zygotic embryogenesis and fertile maize plants. *Plant Cell* **5**:739–746.
- Li, J., Blue, R., Zeitler, B., Strange, T.L., Pearl, J.R., Huizinga, D.H., Evans, S., Gregory, P.D., Urnov, F.D., and Petolino, J.F.** (2013). Activation domains for controlling plant gene expression using designed transcription factors. *Plant Biotechnol. J.* **11**:671–680.
- Li, X., Meng, D., Chen, S., Luo, H., Zhang, Q., Jin, W., and Yan, J.** (2017). Single nucleus sequencing reveals spermatid chromosome fragmentation as a possible cause of maize haploid induction. *Nat. Commun.* **8**:991.
- Li, Y., Lin, Z., Yue, Y., Zhao, H., Fei, X., Lizhu, E., Liu, C., Chen, S., Lai, J., and Song, W.** (2021). Loss-of-function alleles of ZmPLD3 cause haploid induction in maize. *Nat. Plants* **7**:1579–1588.
- Liu, C., Li, X., Meng, D., Zhong, Y., Chen, C., Dong, X., Xu, X., Chen, B., Li, W., Li, L., et al.** (2017). A 4-bp insertion at *ZmPLA1* encoding a putative phospholipase A generates haploid induction in Maize. *Mol. Plant* **10**:520–522.
- Liu, C., Zhong, Y., Qi, X., Chen, M., Liu, Z., Chen, C., Tian, X., Li, J., Jiao, Y., Wang, D., et al.** (2020). Extension of the *in vivo* haploid induction system from diploid maize to hexaploid wheat. *Plant Biotechnol. J.* **18**:316–318.
- Marinho, H.S., Real, C., Cyrne, L., Soares, H., and Antunes, F.** (2014). Hydrogen peroxide sensing, signaling and regulation of transcription factors. *Redox Biol.* **2**:535–562.
- Maryenti, T., Ishii, T., and Okamoto, T.** (2021). Development and regeneration of wheat–rice hybrid zygotes produced by *in vitro* fertilization system. *New Phytol.* **232**:2369–2383.
- Peng, X.B., Sun, M.X., and Yang, H.Y.** (2005). A novel *in vitro* system for gamete fusion in maize. *Cell Res.* **15**:734–738.
- Qi, L.S., Larson, M.H., Gilbert, L.A., Doudna, J.A., Weissman, J.S., Arkin, A.P., and Lim, W.A.** (2013). Repurposing CRISPR as an RNA-guided platform for sequence-specific control of gene expression. *Cell* **152**:1173–1183.
- Steffen, J.G., Kang, I.-H., Macfarlane, J., and Drews, G.N.** (2007). Identification of genes expressed in the Arabidopsis female gametophyte. *Plant J.* **51**:281–292.
- Sun, G., Geng, S., Zhang, H., Jia, M., Wang, Z., Deng, Z., Tao, S., Liao, R., Wang, F., Kong, X., et al.** (2022). Matrilineal empowers wheat pollen with haploid induction potency by triggering postmitosis reactive oxygen species activity. *New Phytol.* **233**:2405–2414.

Parthenogenesis induction in maize

- Tanenbaum, M.E., Gilbert, L.A., Qi, L.S., Weissman, J.S., and Vale, R.D.** (2014). A protein-tagging system for signal amplification in gene expression and fluorescence imaging. *Cell* **159**:635–646.
- Toda, E., Koiso, N., Takebayashi, A., Ichikawa, M., Kiba, T., Osakabe, K., Osakabe, Y., Sakakibara, H., Kato, N., and Okamoto, T.** (2019). An efficient DNA- and selectable-marker-free genome-editing system using zygotes in rice. *Nat. Plants* **5**:363–368.
- Vauterin, M., Frankard, V., and Jacobs, M.** (1999). The *Arabidopsis thaliana* *dhdps* gene encoding dihydrodipicolinate synthase, key enzyme of lysine biosynthesis, is expressed in a cell-specific manner. *Plant Mol. Biol.* **39**:695–708.
- Wang, N., Xia, X., Jiang, T., Li, L., Zhang, P., Niu, L., Cheng, H., Wang, K., and Lin, H.** (2022). In planta haploid induction by genome editing of DMP in the model legume *Medicago truncatula*. *Plant Biotechnol. J.* **20**:22–24.

Plant Communications

- Yao, L., Zhang, Y., Liu, C., Liu, Y., Wang, Y., Liang, D., Liu, J., Sahoo, G., and Kelliher, T.** (2018). OsMATL mutation induces haploid seed formation in indica rice. *Nat. Plants* **4**:530–533.
- Zhong, Y., Chen, B., Li, M., Wang, D., Jiao, Y., Qi, X., Wang, M., Liu, Z., Chen, C., Wang, Y., et al.** (2020). A DMP-triggered *in vivo* maternal haploid induction system in the dicotyledonous *Arabidopsis*. *Nat. Plants* **6**:466–472.
- Zhong, Y., Chen, B., Wang, D., Zhu, X., Li, M., Zhang, J., Chen, M., Wang, M., Riksen, T., Liu, J., et al.** (2022). *In vivo* maternal haploid induction in tomato. *Plant Biotechnol. J.* **20**:250–252.
- Zhong, Y., Liu, C., Qi, X., Jiao, Y., Wang, D., Wang, Y., Liu, Z., Chen, C., Chen, B., Tian, X., et al.** (2019). Mutation of ZmDMP enhances haploid induction in maize. *Nat. plants* **5**:575–580.